Electronic Supplementary Information

Stable Diarylnitroxide Diradical with Triplet Ground State

Andrzej Rajca*, Kouichi Shiraishi, Suchada Rajca

Department of Chemistry, University of Nebraska, Lincoln, NE 68588-0304.

E-mail address: arajca1@unl.edu

Table of Contents

1.   Complete reference 16.

16.   M. J. Frisch, G. W. Trucks, H. B. Schlegel, G. E. Scuseria, M. A. Robb, J. R. Cheeseman, J. A. Montgomery Jr., T. Vreven, K. N. Kudin, J. C. Burant, J. M. Millam, S. S. Iyengar, J. Tomasi, V. Barone, B. Mennucci, M. Cossi, G. Scalmani, N. Rega, G. A. Petersson, H. Nakatsuji, M. Hada, M. Ehara, K. Toyota, R. Fukuda, J. Hasegawa, M. Ishida, T. Nakajima, Y. Honda, O. Kitao, H. Nakai, M. Klene, X. Li, J. E. Knox, H. P. Hratchian, J. B. Cross, C. Adamo, J. Jaramillo, R. Gomperts, R. E. Stratmann, O. Yazyev, A. J. Austin, R. Cammi, C. Pomelli, J. W. Ochterski, P. Y. Ayala, K. Morokuma, G. A. Voth, P. Salvador, J. J. Dannenberg, V. G. Zakrzewski, S. Dapprich, A. D. Daniels, M. C. Strain, O. Farkas, D. K. Malick, A. D. Rabuck, K. Raghavachari, J. B. Foresman, J. V. Ortiz, Q. Cui, A. G. Baboul, S. Clifford, J. Cioslowski, B. B. Stefanov, G. Liu, A. Liashenko, P. Piskorz, I. Komaromi, R. L. Martin, D. J. Fox, T. Keith, M. A. Al-Laham, C. Y. Peng, A. Nanayakkara, M. Challacombe, P. M. W. Gill, B. Johnson, W. Chen, M. W. Wong, C. Gonzalez and J. A. Pople, *Gaussian 03*, Revision E.01 (Gaussian, Wallingford, CT, 2004).

2.   General procedures and materials.

Per-deuterated solvents for NMR spectroscopy were obtained from Cambridge Isotope Laboratories. All other commercially available chemicals were obtained from Aldrich, unless indicated otherwise.

Solution of DMDO in acetone (ca. 0.05–0.10 M) was prepared as described previously.[S1] Extraction and concentration into a solution in dichloromethane/acetone (~6:1, ca. 0.35–0.1 M) was carried out as reported in the literature.[S2]   Concentrations of DMDO were periodically determined by tritrations carried out in duplicate with triphenylphoshine; molar ratio of unreacted phosphine to the corresponding oxide was determined by ^{1}H NMR spectroscopy.[S3]

Column chromatography was carried out on TLC grade silica gel (Aldrich), using 0–20 psig pressure. Preparative TLC (PTLC) was carried out using Analtech silica plates (tapered with a preadsorbent zone). For selected separations, silica gel was deactivated by treatment with a solution of triethylamine in pentane. Standard techniques for synthesis under inert atmosphere, using Schlenk glassware and gloveboxes (Mbraun and Vacuum Atmospheres), were employed. NMR spectra were obtained using Bruker spectrometer (^{1}H, 400 MHz) using acetone-d_6 and chloroform-d (CDCl$_3$) as solvent. The 500 MHz instrument was equipped with a cryoprobe. The ^{1}H chemical shift references were as follows: acetone-d_5, 2.05 ppm and CDCl$_3$, 7.26 ppm. IR spectra were obtained using a Nicolet Avatar 360 FT-IR instrument, equipped with an ATR sampling accessory (Spectra Tech, Inc.). A few drops of the compound in CH$_2$Cl$_2$ were applied to the surface of a ZnSe ATR plate horizontal parallelogram (45°, Wilmad). After the solvent evaporated, the spectrum was acquired (4-cm^{-1} resolution).

UV-vis spectra were obtained on Shimadzu (UV-2401PC) spectrophotometer. Only one concentration was used; thus, the values of ε_{max} were very approximate.

Purification, drying, and titration of *m*-CPBA. *m*-CPBA was dissolved in benzene and washed with buffer solution (pH = 7.4, NaH$_2$PO$_4$/NaOH). The organic layer was dried over MgSO$_4$ (or Na$_2$SO$_4$), filtered, and solvent removed. White needle crystals were obtained by recrystallization from dichloromethane at 0 °C. The *m*-CPBA was then dried under 1 mTorr vacuum with molecular sieves (3 Å) overnight. (Molecular sieves were pre-activated at 200−210 °C under 1 mTorr vacuum overnight). Titration of *m*-CPBA was performed using the following procedure. *m*-CPBA was dissolved in CH$_3$COOH (minimum volume) and then transferred to a H$_2$O/CH$_3$COOH solution (N$_2$ bubbling for 5 min before transfer) under N$_2$ flow. An aqueous
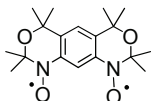
solution of KI (excess) was added to the *m*-CPBA solution (obtained orange solution) and heated to

reflux for 15 min. The solution was then cooled to ambient temperature and titrated with an

aqueous solution of $Na_2S_2O_3$.

3. EPR spectroscopy.

CW X-band EPR spectra for diarylnitroxide diradical **2** were acquired on Bruker EMX

instrument, equipped with a frequency counter. Temperature was controlled with either nitrogen

flow system (130–300 K) or liquid nitrogen dewar insert (~80 K). The samples were contained in

either 4-mm EPR quartz tubes or 5-mm SQUID sample tubes. All spectra were obtained with the

oscillating magnetic field perpendicular (TE$_{102}$) to the swept magnetic field. The *g*-values were

referenced using DPPH (*g* = 2.0037, powder, Aldrich).

The WINEPR SimFonia program (Version 1.25, Bruker) was used for spectral simulations of

nitroxide diradical **2** in rigid matrices (Table S1).

Table S1. EPR spectral parameters for diarylnitroxide diradical **2** and planar alkylarylnitroxide

diradical.

diradical	solvent	T (K)	ν^a (GHz)	g_x	g_y	g_z	$|D/hc|/10^{-4}$ (cm^{-1})	$|E/hc|/10^{-4}$ (cm^{-1})	$|A_{yy}/2hc|/10^{-4}$ (^{14}N, cm^{-1})
2	toluene	~80[b]	9.4246	2.0074	2.0016	2.0045	122.3	14.4	10.6
		140[c]	9.6545	2.0076	2.0020	2.0047	122.5	14.0	10.6
	2-MeTHF	140[d]	9.6504	2.0084	2.0024	2.0052	130	15.5	11.5

[a] Microwave frequencies (ν) are dependent on the cavity type and the sample. [b] Sample label: KS373-3; simulation label: KS373sm5. [c] Sample label: KS718-1-recryst1; simulation label: smKS750. [d] ref S4.

4. SQUID magnetometry.

5-Tesla AC/DC SQUID magnetometer, with continuous temperature control and operating in the DC-mode, was used.   All solution samples and some solid samples were contained in home-made 5-mm O.D. EPR quality quartz tubes, modified to possess a thin bottom, which is 6 cm from the end of the tube (referred to as "SQUID tubes").[S4,S5]

For solid state samples, diradical **2** (5.13 mg or 12.32 mg) was loaded to the 3-piece gelatine capsule.   Following the measurements, the capsule was emptied (for the larger sample, 2.20 mg was retained), and then identical sequences of measurements was carried out for the point-by-point correction for diamagnetism.   Additional correction was based upon Pascal constants: χ_{dia} = -3.27×10^{-4} emu mol^{-1}.   Other samples (0.66–6.14 mg) were measured using similar procedure but without point-by-point correction.

For another set of solid state samples, diradical **2** was loaded to the SQUID tube, placed under vacuum, and then flame sealed under partial pressure of helium gas.   Following the measurements, the SQUID sample tube was opened and cleaned, and then identical sequences of measurements were carried out for the point-by-point correction for diamagnetism; additional corrections were based upon Pascal constants.

For solution samples, diradical **2** (0.53 mg for the THF sample in Figure 4, text) was loaded into the SQUID tube, and then placed under vacuum.   THF or dichloromethane were vacuum transferred, and after the tube was flame sealed under vacuum, the samples were carefully inserted to the magnetometer, as described elsewhere.[S4]   Correction for diamagnetism was implemented by extrapolation of the χ vs. $1/T$ plots in the 70–140 K temperature range (R^2 = 0.9999).

Numerical curve fitting for magnetic data was carried out with the SigmaPlot for Windows software package.   The reliability of a fit is measured by the parameter dependence, which is defined as follows: *dependence = 1 − ((variance of the parameter, other parameters constant)/(variance of the parameter, other parameters changing))*.   Values close to 1 indicate overparametrized fit.

M vs. *H* data in THF at low temperatures (T = 1.8, 3, 5 K) were analyzed with Brillouin functions (with mean-field parameter, θ).   For the THF sample in Figure 4 (text), numerical fits gave S = 0.99 (i.e., S = 1.0), θ = −0.15 K, with the parameter dependence of 0.56, 0.84, 0.97 at 1.8, 3, and 5 K, respectively.

5.   Oxidation of diamine 3 with DMDO.
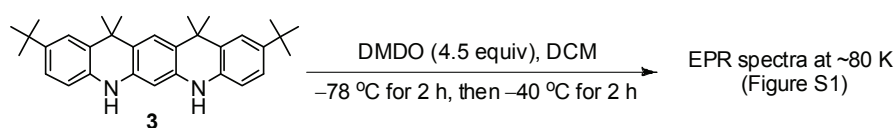
Low-temperature oxidation of diamine 3 with EPR monitoring.   Dichloromethane (~0.2 mL) was added by vacuum transfer to diamine **3** (1.47 mg, 1 equiv) in a 4-mm O.D. EPR quartz sample tube equipped with high-vacuum stopcock.   Subsequently, DMDO (~0.10 M solution in dichloromethane, ~0.14 mL, ~4.5 equiv) was vacuum transferred.   After stirring for 2 h at −78 °C, EPR spectrum for the dark reaction mixture were obtained at ~80 K, as illustrated in Figure S1 (KS281-1).   After recording the EPR spectrum, the sample tube was kept for 2 h at −40 °C, and then for the red homogenious reaction mixture, another set EPR spectra was obtained at ~80 K as illustrated in Figure S1 (KS281-4).

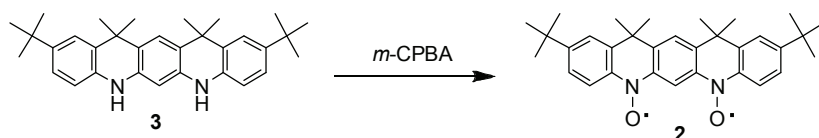## 6. Oxidation of diamine 3 with *m*-CPBA: characterization of nitroxide diradical 2.

Table S2. Characterization of nitroxide diradical **2**.

Sample label for nitroxide diradical **2**	EPR Label (Figure)	SQUID Label (Figure)	SQUID Description	^{1}H NMR Label (Figure)
KS357-3	KS373[*1] (Fig. 3, text)	-	-	KS357-3 (Fig. S10, ESI)
KS410-4	KS419/KS410 (Fig. S6, ESI) KS424r1r2r3[*2] (Fig. S7, ESI)	KS424r2H (Fig. 4, text)	Solution in THF	KS410-4 (Fig. S11, ESI)
KS436-1	KS443/KS436-1 KS447/KS436-1[*3]	KS443 KS446 KS447	Solid/capsule Solution in DCM Solid/SQUID tube	KS436-1 (Fig. S11, ESI) KS447[*3]
KS450-1[*4]	KS450-1-1 (Fig. S5, ESI)	KS451r1G (Fig. 5, text)	Solid/capsule, (point-by-point)	-
KS718-1-recryst1	KS750r1/r2[*1] (Fig. S4, ESI)	KS754r1G (Fig. S8, ESI)	Solid/capsule	-
KS744-1-recryst1	KS764[*1] (Fig. S9, ESI)	KS767	Solid/capsule	-
KS1054-2	KS1058 KS1054-2r5r6 (Fig. S2, ESI)	KS1066	Solid/SQUID tube no background	-
KS1116-2	KS1117 KS1142r1/r2 (Fig. S2, ESI)	KS1139rF (Fig. S3, ESI)	Solid/capsule, (point-by-point)	-

[*1] EPR tube was flame-sealed. [*2] EPR spectra taken directly in the SQUID tube. [*3] EPR and ^{1}H NMR spectra after SQUID stdies. [*4]

UV/vis (*n*-heptane): λ_{max}/nm (ε_{max}/L mol^{-1} cm^{-1}) = 285 (~5.1 × 10^3), 311 (~1.1 × 10^4), 330 (~1.3 × 10^4), 418 (~1 × 10^3), 442 (~1.0 ×

10^3), 474 (~8 × 10^2) (Fig. S12, ESI, label: KS450-1_r1).

Nitroxide diradical 2: general procedure with partial purification (KS1116). m-CPBA (3.4 mL of 0.39 M solution in dichloromethane, 2 equiv) was slowly added to diamine **3** (KS911-1, MW = 452.6, 300.0 mg, 0.663 mmol) in DCM (44 mL, 0.015 M) at 0 °C under nitrogen atmosphere. After 20 min at 0 °C, the second portion of m-CPBA (3.4 mL of 0.39 M solution in dichloromethane, 2 equiv) was slowly added to the resultant pink-brown homogenous reaction mixture.   After 40 min at 0 °C, the third portion of m-CPBA (3.4 mL of 0.39 M solution in dichloromethane, 2 equiv) was added, and then the reaction mixture was stirred for 2.5 h at 0 °C. The obtained dark yellow solution was concentrated to provide crude product (KS1116-crude, 929.0 mg).   Rapid filtration through silica gel column (deactivated silica, dichloromethane/ether, 9:1) gave orange fraction containing nitroxide diradical.   The orange fraction was concentrated, to provide nitroxide diradical as green powder (79.3 mg, 25%, label: KS1116-2).   In another reaction (label: KS1054) on the 200-mg scale, 48.7 mg (23%, label: KS1054-2) of nitroxide diradical was obtained from diamine **3** (200.0 mg, 0.442 mmol).

Nitroxide diradical 2: two representative procedures with complete purifications (KS357 and KS410).   The crude reaction mixture (KS357), obtained from diamine **3** (39.4 mg) using the general procedure, was purified by two consecutive PTLC (dichloromethane/ether, 98:2).   The orange fraction was collected, and then by recrystallized from dichloromethane/methanol at –20 °C, to provide diradical **2** as green solid: 2.4 mg (6%) (label: KS357-3).

The crude reaction mixture (KS-410), obtained from diamine **3** (97.3 mg) using the general procedure (vacuum transferred dichloromethane, 19.5 mL), was filtered through silica plug at room temperature (eluent: benzene/ether, 95:5, R_f = 0.4).   Subsequently, two consecutive PTLC were carried out.   Orange fraction (slightly higher R_f-value than the adjacent "green fraction") was

collected. After the first PTLC (benzene/ether, 98:2), diradical **2** with a small admixture of

monoradical (7.3 mg, label: KS410-2) was obtained. After the second PTLC

(dichloromethane/ether, 98:2), diradical **2** was obtained as green solid: 4.8 mg (5%, label: KS410-4)

(EPR spectra: Figure S6).

7. Reduction of nitroxide radicals to the corresponding amines.

Reduction of 4,4'-di-*tert*-butyl-diphenylnitroxide radical (KS842).
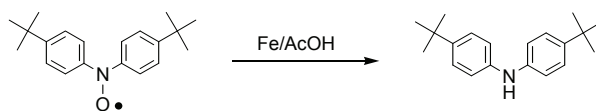
Acetic acid (EMD, 50 μl) and Fe (Acros, MW = 55.8, 0.8 mg, 0.0143 mmol) was added to

4,4'-di-*tert*-butyl-diphenylnitroxide radical[S3] (0.81 mg, 2.73 μmol); the resultant orange solution

was stirred for 10 min at 50 °C, and then for 3 h at room temperature. The reaction mixture was

added to saturated aqueous K_2CO_3, extracted with dichloromethane, and dried over Na_2SO_4.

Removal of solvents gave crude reaction mixture (~1.2 mg, label: KS842-crude), for which [1]H

NMR spectrum was obtained: ^{1}H NMR (400 MHz, CDCl₃): δ = 7.274 (d, J = 8.8 Hz, 4H), 7.003 (d,

J = 8.4 Hz, 4H), 5.574 (brs, 1H), 1.307 (s, 18H). ^{1}H NMR spectrum for independently prepared

reference sample of 4,4'-di-*tert*-butylphenylamine (label: KS187-cryst1): ^{1}H NMR (400 MHz,

CDCl₃): δ = 7.279 (d, J = 8.4 Hz, 4H), 7.006 (d, J = 8.4 Hz, 4H), 5.571 (brs, 1H), 1.313 (s, 18H).

Reduction of nitroxide diradical 2 to diamine 3 (KS844).
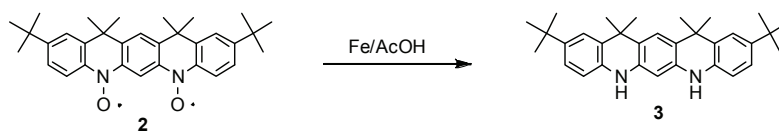
Acetic acid (EMD, 200 μl) and Fe (Acros, MW = 55.8, 0.8 mg, 0.0143 mmol) was added to

nitroxide diradical **2** (0.54 mg, 1.1 μmol, KS450-1); characterization of this sample of diradical is

summarized in Table S2.   The resultant orange solution was stirred for 10 min at 50 °C, and then

for 3 h at room temperature.   Subsequently, the reaction mixture was added to saturated aqueous

K_2CO_3, extracted with dichloromethane, and dried over Na_2SO_4.   Removal of solvents gave crude

reaction mixture (~0.6 mg, label: KS844-crude); the ^{1}H NMR spectrum showed the diamine **3** with

a small admixture of impurities.   ^{1}H NMR (400 MHz, acetone-d_6): diamine **3**, δ = 7.760 (s, 2H of

NH), 7.429 (d, J = 2.4 Hz, 2H), 7.404 (s, 1H), 7.013 (dd, J = 2.0, 8.4 Hz, 2H), 6.680 (d, J = 8.4 Hz,

2H), 6.224 (s, 1H), 1.574 (s, 12H), 1.292 (s, 18H); impurities (aromatic region), 8.59 (d, 0.05H),

7.90 (s, 0.03H), 7.10 (d, 0.14H), 7.55 (m, 0.38H), 7.43 (m, 0.12H), 7.25 (dd, 0.09H), 7.18 (d,

0.09H), 6.96 (dd, 0.30H), 6.57 (d, 0.08H).   Purification by PTLC (benzene/pentane, 8:2), gave

diamine **3** as white powder (0.43 mg, 80%) (label: KS844-1).   ^{1}H NMR (400 MHz, acetone-d_6): δ

= 7.765 (s, 2H of NH), 7.429 (d, J = 2.4 Hz, 2H), 7.404 (s, 1H), 7.013 (dd, J = 2.0, 8.4 Hz, 2H),

6.681 (d, J = 8.4 Hz, 2H), 6.224 (s, 1H), 1.573 (s, 12H), 1.291 (s, 18H).

8.   Supporting figures.
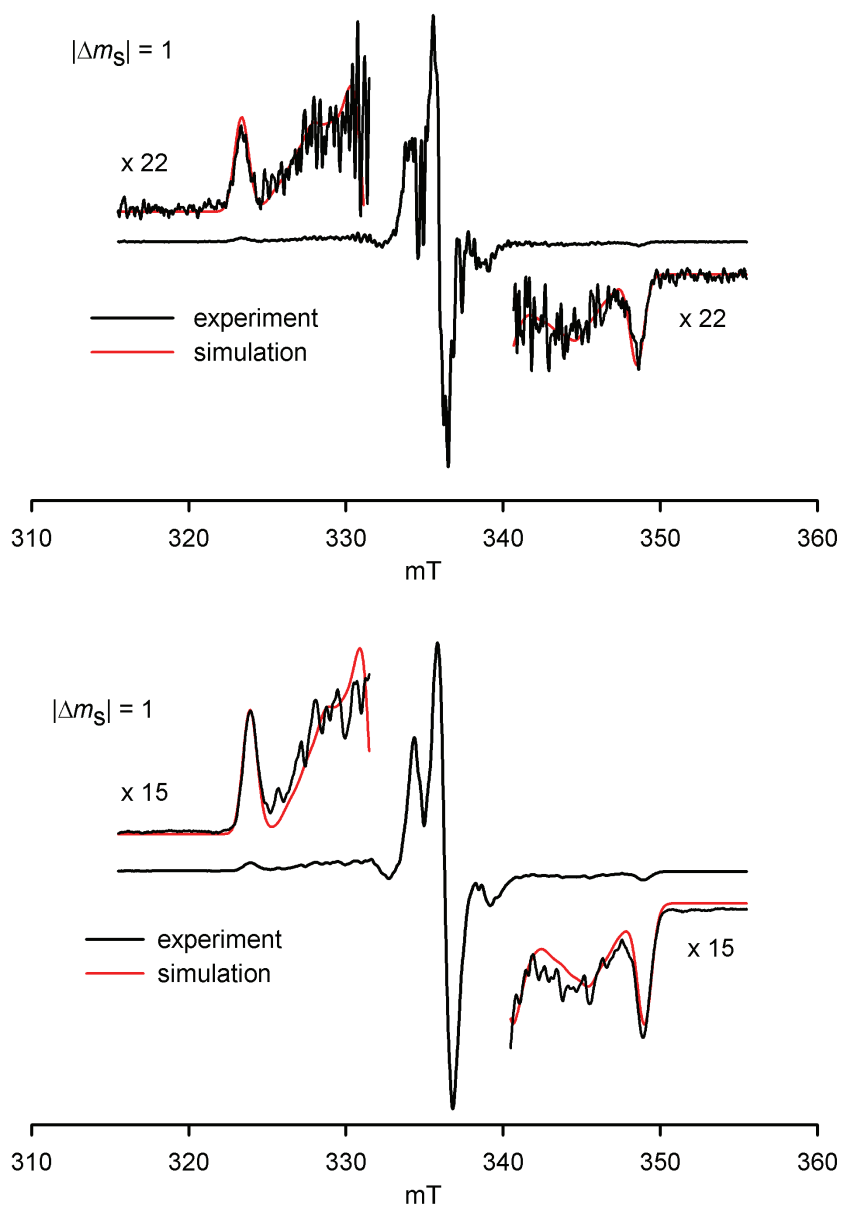
Figure S1.   EPR spectra (X-band, 77 K) for reaction mixtures for low-temperature oxidation of diamine **3** with DMDO.   Top plot: spectrum taken after 2 h at −78 °C, ν = 9.4183 GHz (label: KS281-1).   Bottom plot: spectrum taken after additional 2 h at −40 °C, $\nu \approx$ 9.42 GHz (label: KS281-4).   The side bands were simulated with the following parameters for the $S = 1$ state: $|D/hc|$ = 11.75 × 10^{-3} cm^{-1}, $|E/hc|$ = 1.3 × 10^{-3} cm^{-1}, $|A_{yy}/2hc|$ = 10.0 × 10^{-4} cm^{-1}, $g_x \approx$ 2.0076, g_y = 2.0020, g_z = 2.0040, Gaussian line (L_x = 1.1, L_y = 1.1, L_z = 0.9 mT) (label: SMdmdo4).

$|\Delta m_s| = 1$, 140 K

$|\Delta m_s| = 2$

162   172   182

$|\Delta m_s| = 1$, 140 K

$|\Delta m_s| = 2$

162   172   182

320   330   340   350   360   370

mT
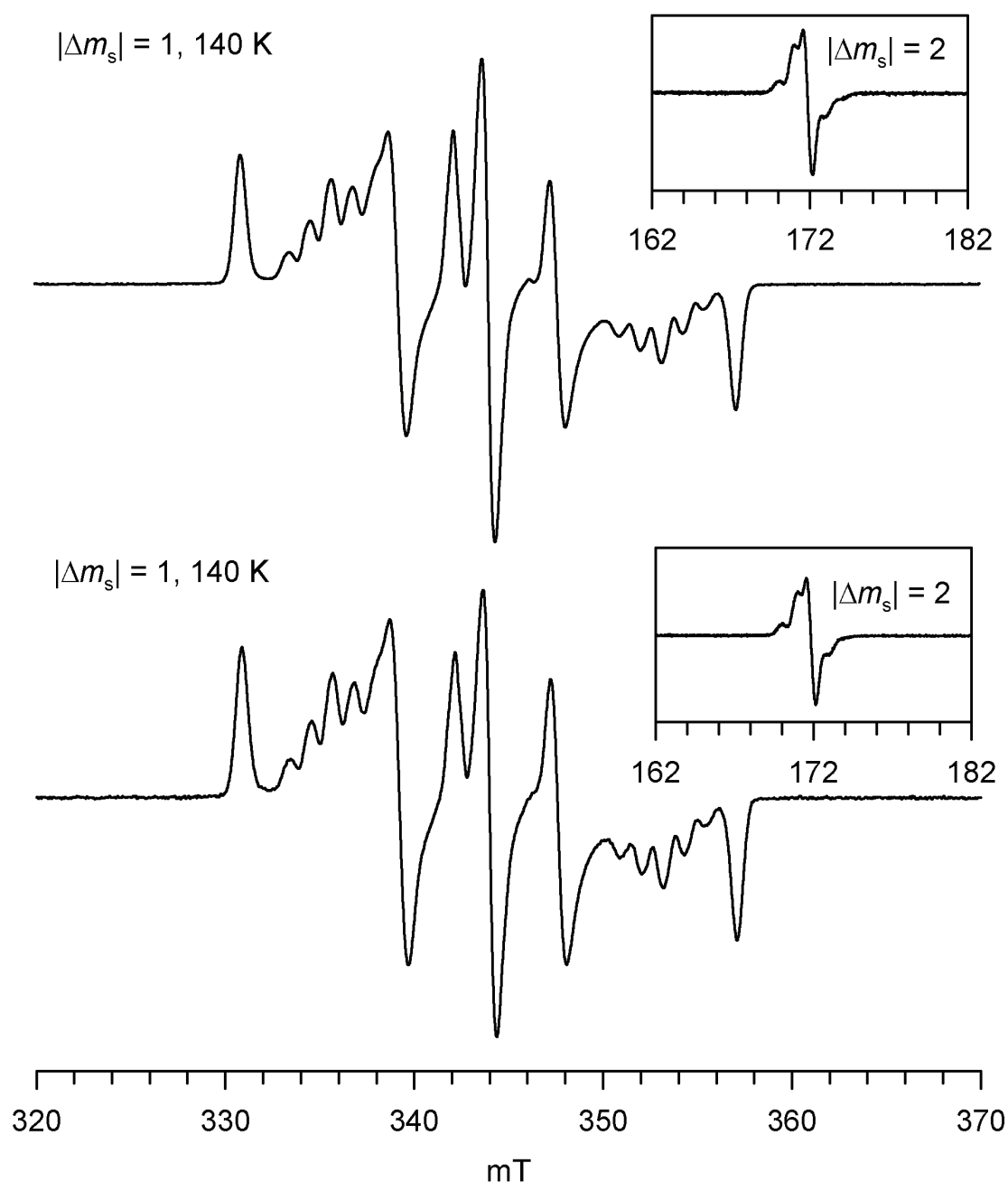
Figure S2. EPR (X-Band, $\nu = 9.652$ and 9.651 GHz) spectra for nitroxide diradical **2** in toluene at 140 K, obtained in ~20% isolated yields from two large-scale reactions. Top spectra (labels: KS1054-2r5/r6) are for the sample KS1054-2 (47.4 mg isolated from the reaction starting with 200 mg of diamine **3**). The bottom spectra (labels: KS1142r1/r2) are for the sample KS1116-2 (79.3 mg isolated from the reaction starting with 300 mg of diamine **3**); the bottom spectra were recorded after SQUID magnetometry (Figure S3).

S13
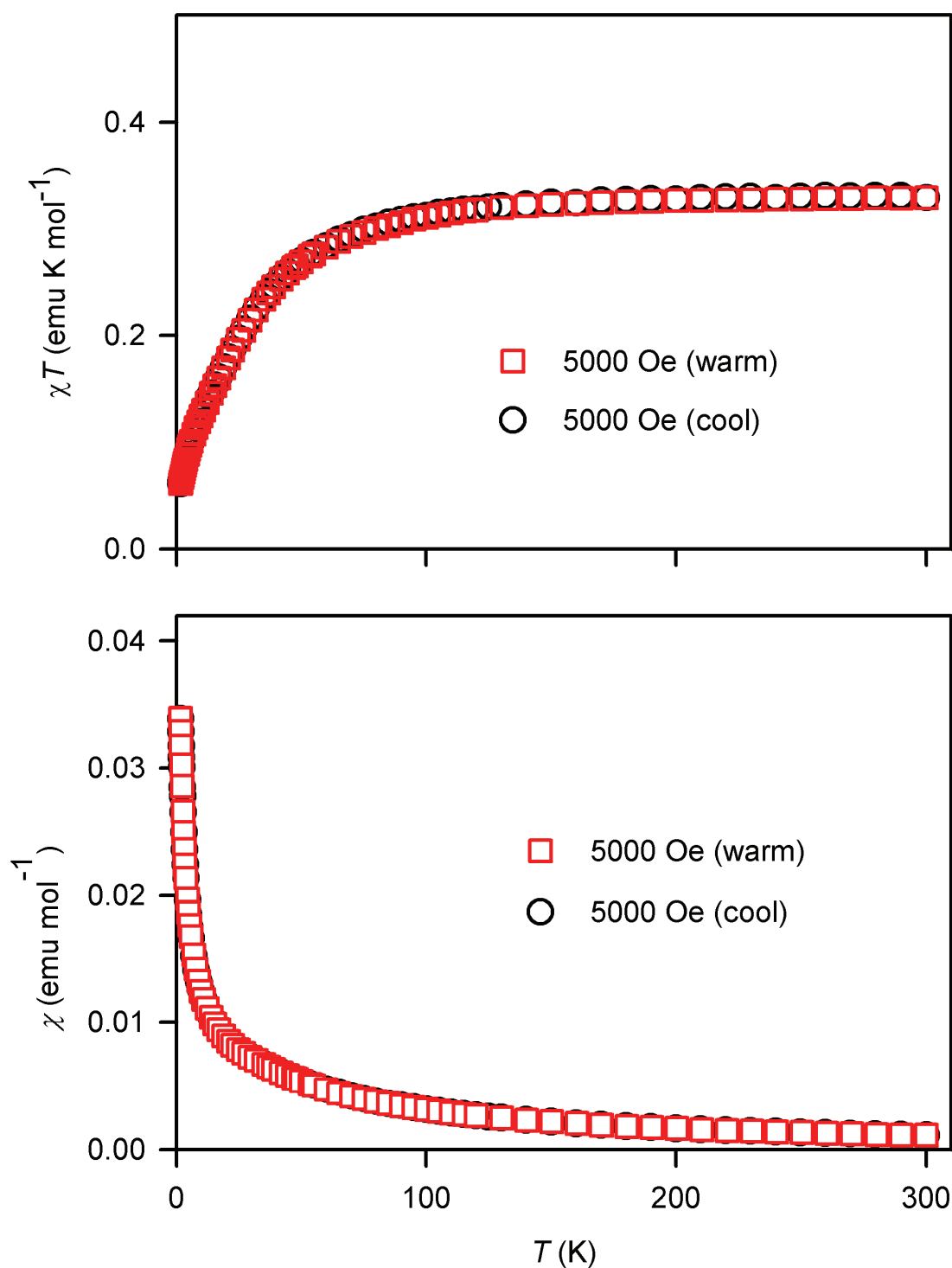
Figure S3. SQUID magnetometry for solid nitroxide diradical **2**: plot of χT vs. T, $\chi T = 0.33$ emu K mol^{-1} at 200–300 K, with the point-by-point background correction and Pascal constant correction (SQUID label: KS1139rF). This sample of **2** is from the large-scale preparation (label: KS1116-2); EPR spectra for this sample are shown in Figure S2 (preceding page).
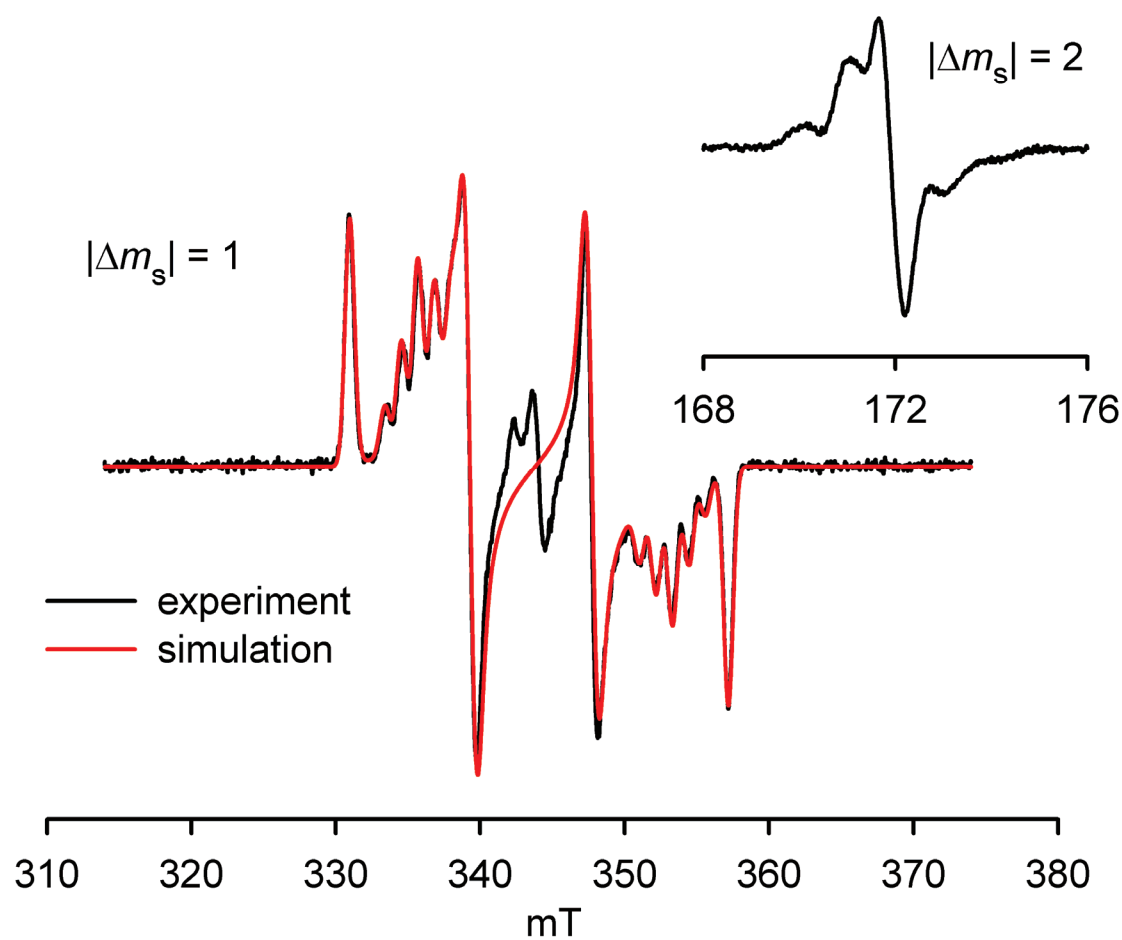
Figure S4. EPR (X-Band, ν = 9.6545 GHz) spectrum of nitroxide diradical **2** (sample label: KS0718-1-recryst1) in toluene at 140 K (KS750r1/r2, smKS750). This is the identical sample (KS0718-1-recryst1) as used for magnetic data (KS754G1) in Figure S8. The spectral simulation of the $|\Delta m_s|$ = 1 region is shown as red trace. The fitting parameters for the spectral simulation to the $S = 1$ state are: $|D/hc| = 1.225 \times 10^{-2}$ cm^{-1}, $|E/hc| = 1.40 \times 10^{-3}$ cm^{-1}, $|A_{yy}/2hc| = 1.06 \times 10^{-3}$ cm^{-1}, $g_x = 2.0076$, $g_y = 2.0020$, $g_z = 2.0047$, Gaussian line ($L_x = 0.75$ mT, $L_y = 0.70$ mT, $L_z = 0.65$ mT). The center lines correspond to an $S = \frac{1}{2}$ (monoradical) impurity.

S15

room temperature

310   320   330   340   350   360

mT

$|\Delta m_s| = 1$, 77 K

310   320   330   340   350   360

mT
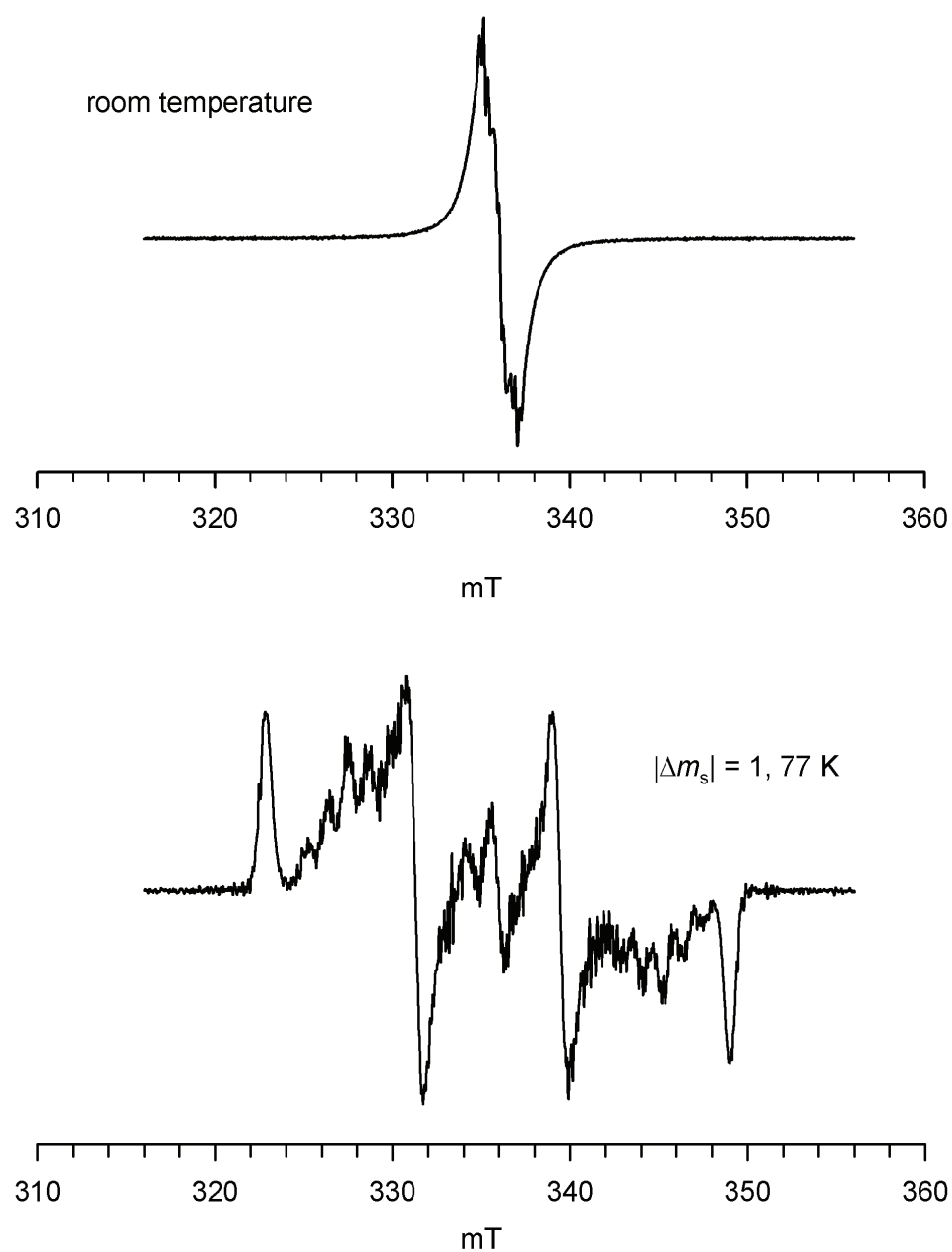
Figure S5. EPR (X-Band) spectra for nitroxide diradical **2** in toluene (sample label: KS450-1).

The top spectrum (v = 9.4299 GHz, 0.204 mW, modulation amplitude of 0.5 Gauss) is obtained at

room temperature (KS450-1-1). The bottom spectrum (v = 9.4241 GHz, 0.0204 mW, modulation

amplitude of 2.0 G) is obtained at 77 K (KS450-1-3). This is the identical sample (KS450-1) as

used for magnetic data in the solid state (KS451r1G) in Figure 5, main text.

S16

Diradical **2** after first PTLC
$|\Delta m_s| = 1$, 77 K

Diradical **2** after final PTLC
(room temperature)

Diradical **2** after final PTLC
$|\Delta m_s| = 1$, 77 K
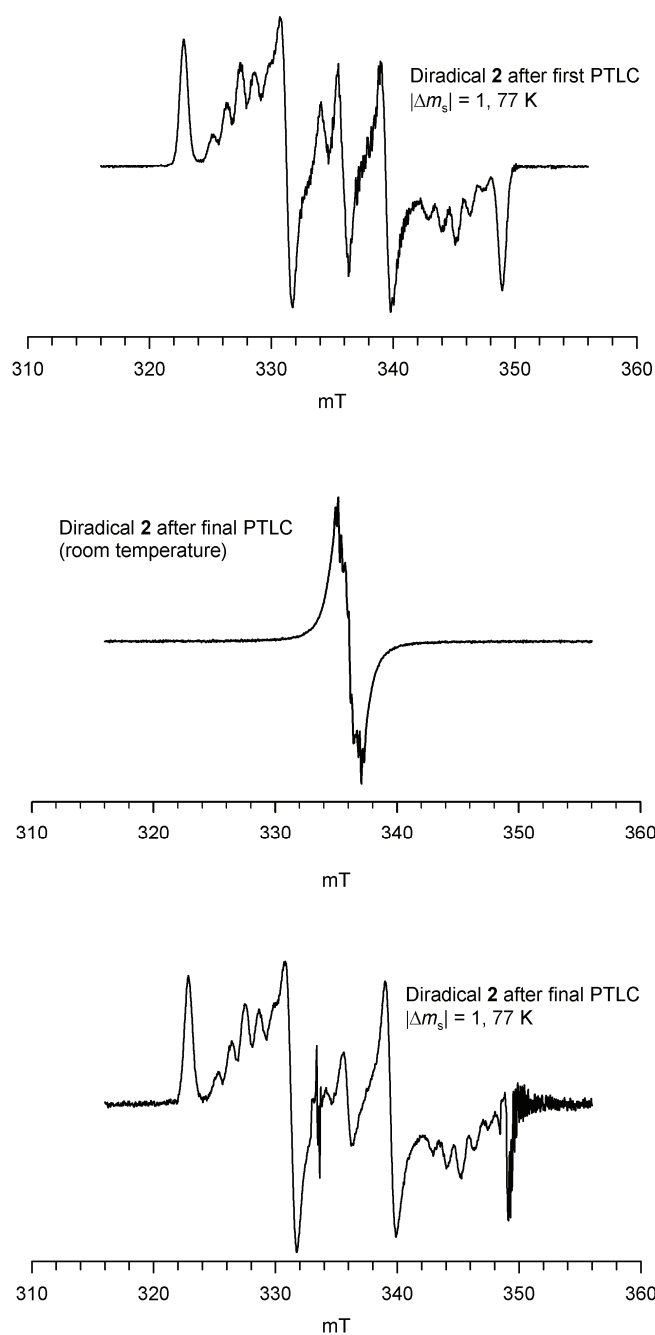
Figure S6. EPR (X-Band) spectra for nitroxide diradical **2** in toluene. The top spectrum (sample label: KS410-2, ν = 9.4227 GHz, 0.0204 mW, modulation amplitude of 2.0 G), the middle spectrum (sample label: KS410-4, ν = 9.4306 GHz, 0.204 mW, modulation amplitude of 0.5 G), and the bottom spectrum (ν = 9.4244 GHz, 0.0204 mW, modulation amplitude of 2.0 G) are obtained at 77 K, room temperature, and 77 K, respectively. The sample KS410-4 is identical to that used for magnetic data in THF (KS424r2H) in Figure 4, main text.

S17
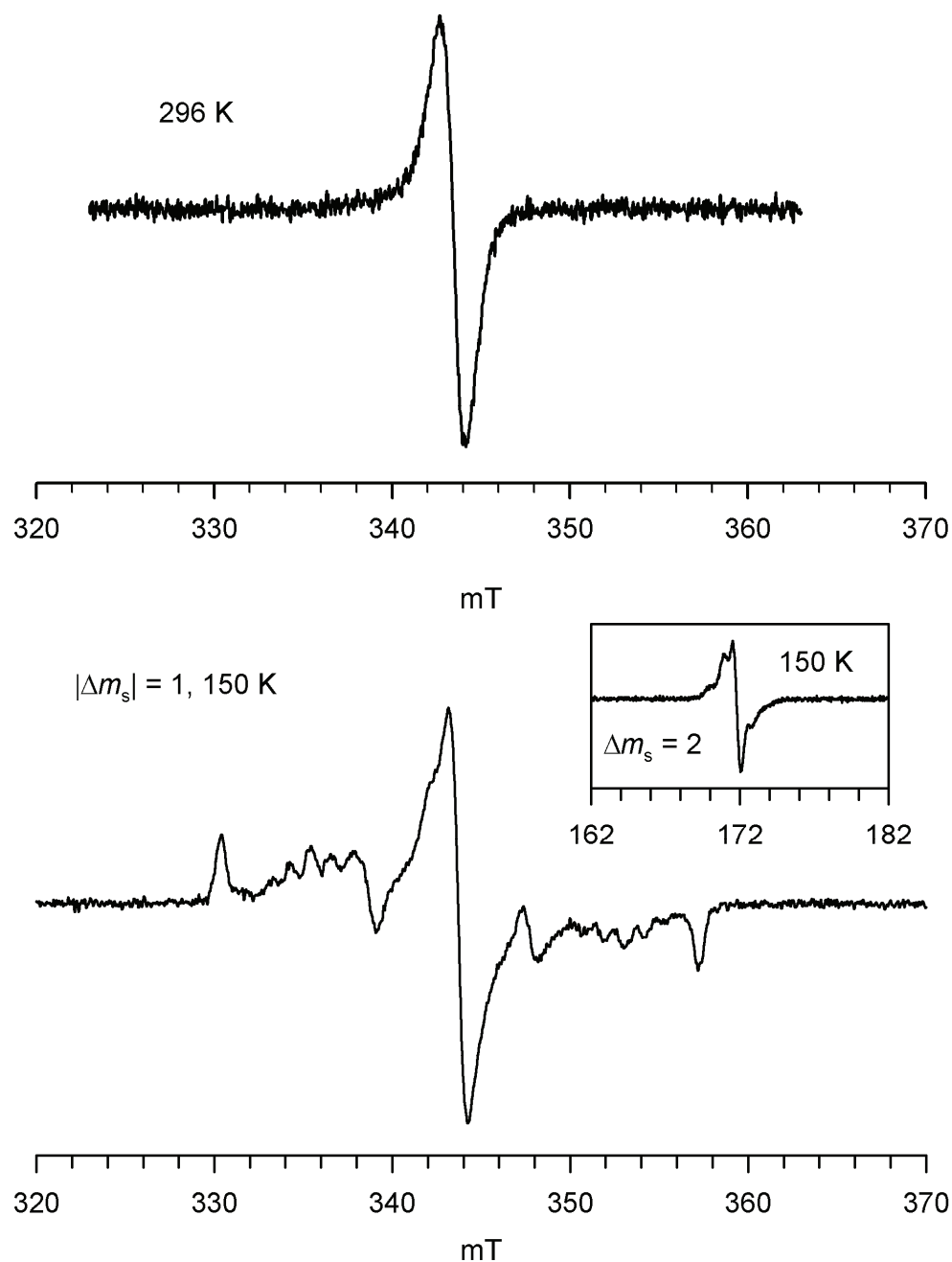
Figure S7. EPR (X-Band) spectra for ~15 mM nitroxide diradical **2** (sample label: KS410-4) in THF, which contained in the flame-sealed SQUID tube, following magnetic data in THF (KS424r2H). The magnetic data are shown in Figure 4 (main text). The top spectrum (ν = 9.6415 GHz, 0.00204 mW, modulation amplitude of 0.5 Gauss) is obtained at 296 K (KS424r1). The bottom spectra (for $|\Delta m_s|$ = 1, ν = 9.6468 GHz, 0.00204 mW, modulation amplitude of 0.5 Gauss) is obtained at 150 K (KS424r2/r3).
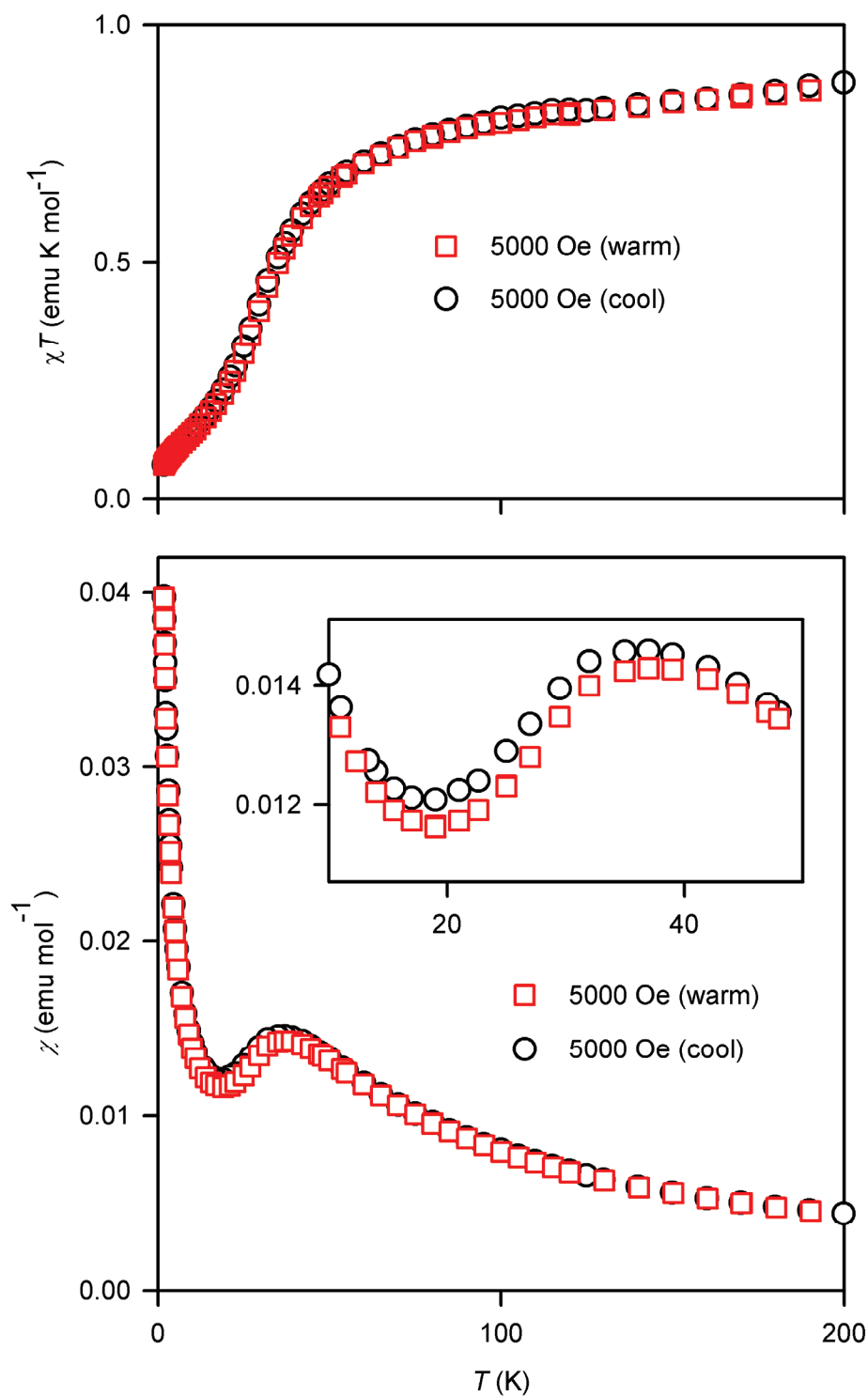
Figure S8. SQUID magnetometry for solid nitroxide diradical **2**: plot of χT vs. T; χT_{max} is at

37–39 K (SQUID label: KS754G1). This is the identical sample of **2** (KS0718-1-recryst1) as used

for EPR spectra (KS750r1/r2) in Figure S4.

room temperature

340   342   344   346   348

mT
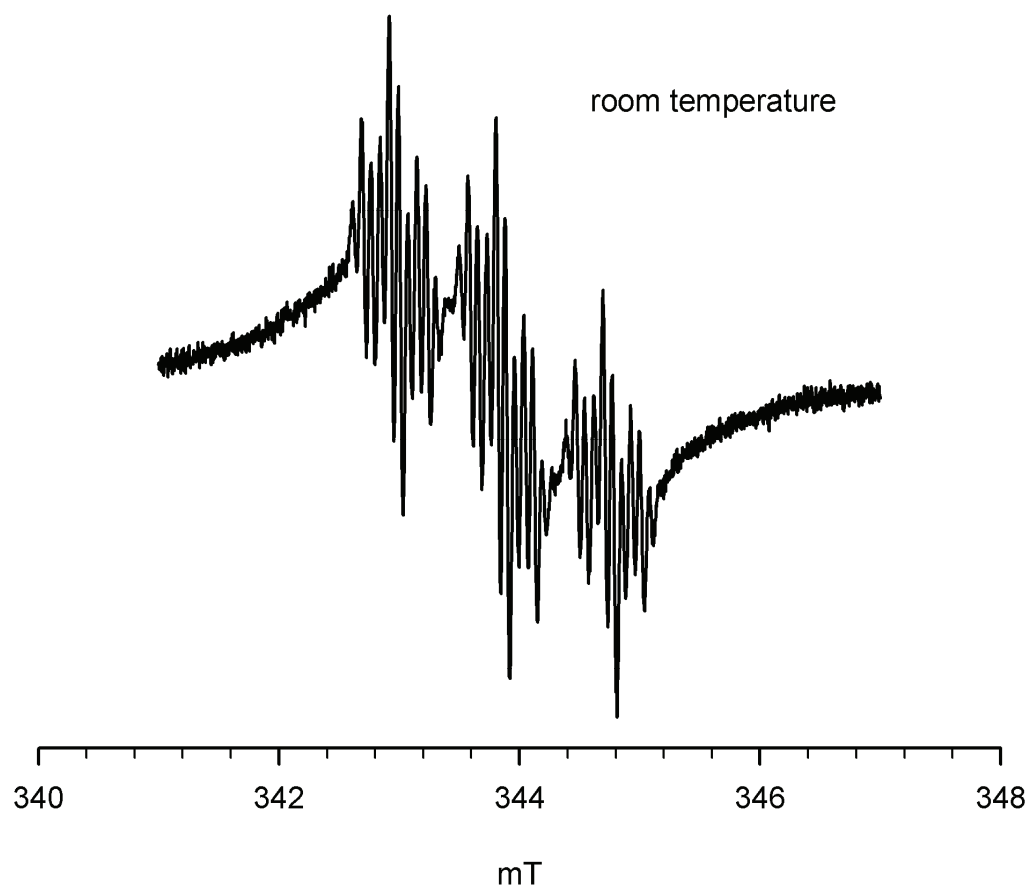
Figure S9. EPR (X-Band, ν = 9.6504 GHz, 2.05 mW, modulation amplitude of 0.2 G) spectrum

nitroxide diradical **2** in toluene at 295 K (sample label: KS744-1, EPR label: KS758r5). The

spectrum is obtained from the sample obtained in ~33% isolated yield in the 60-mg scale reaction.

The sharp peaks correspond to a monoradical by-product.

```
ks-03-057-3 in CDCl3
LB = 5.0 Hz
```
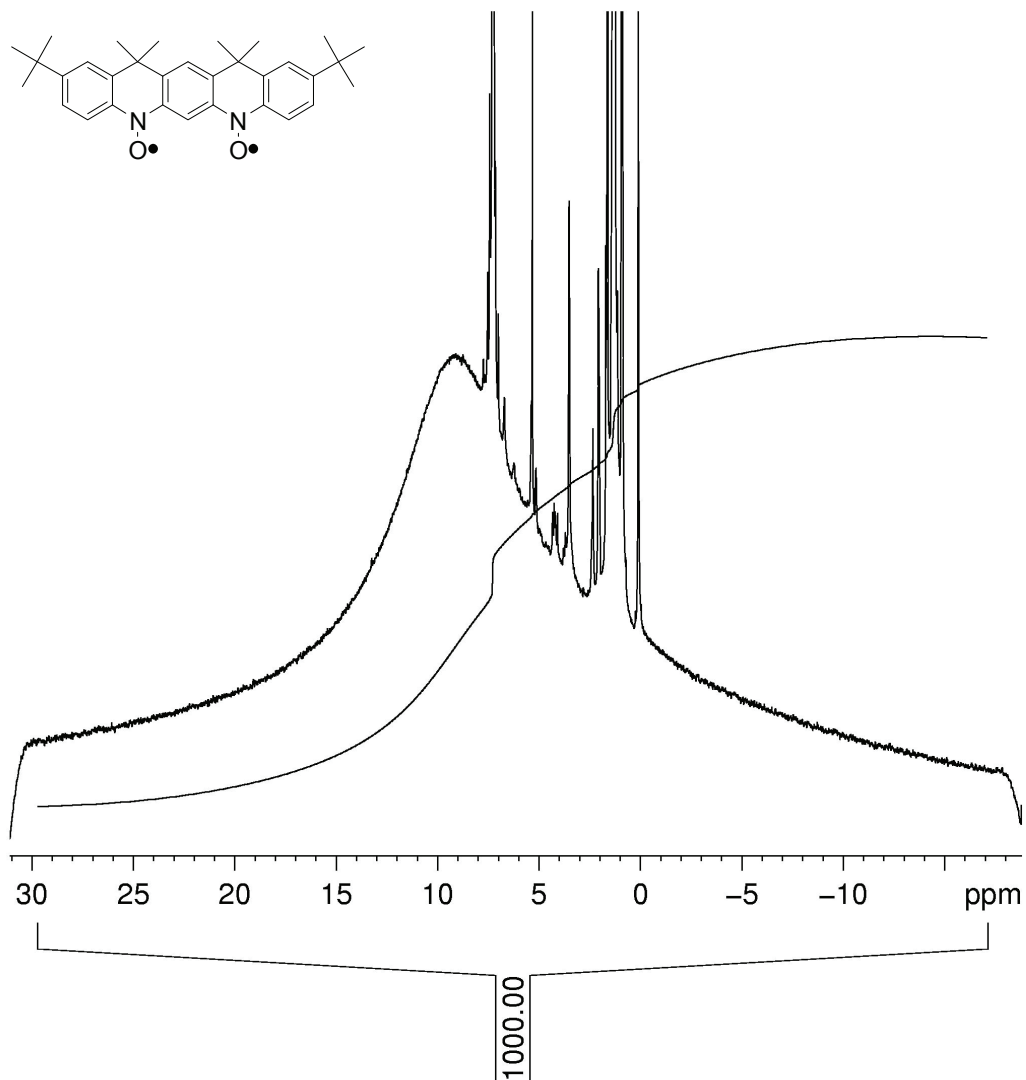

Figure S10a. ^{1}H NMR (400 MHz, CDCl$_3$) spectrum of nitroxide diradical **2** (KS357-3).

```
ks-03-057-3 total Integration set = 1000
```
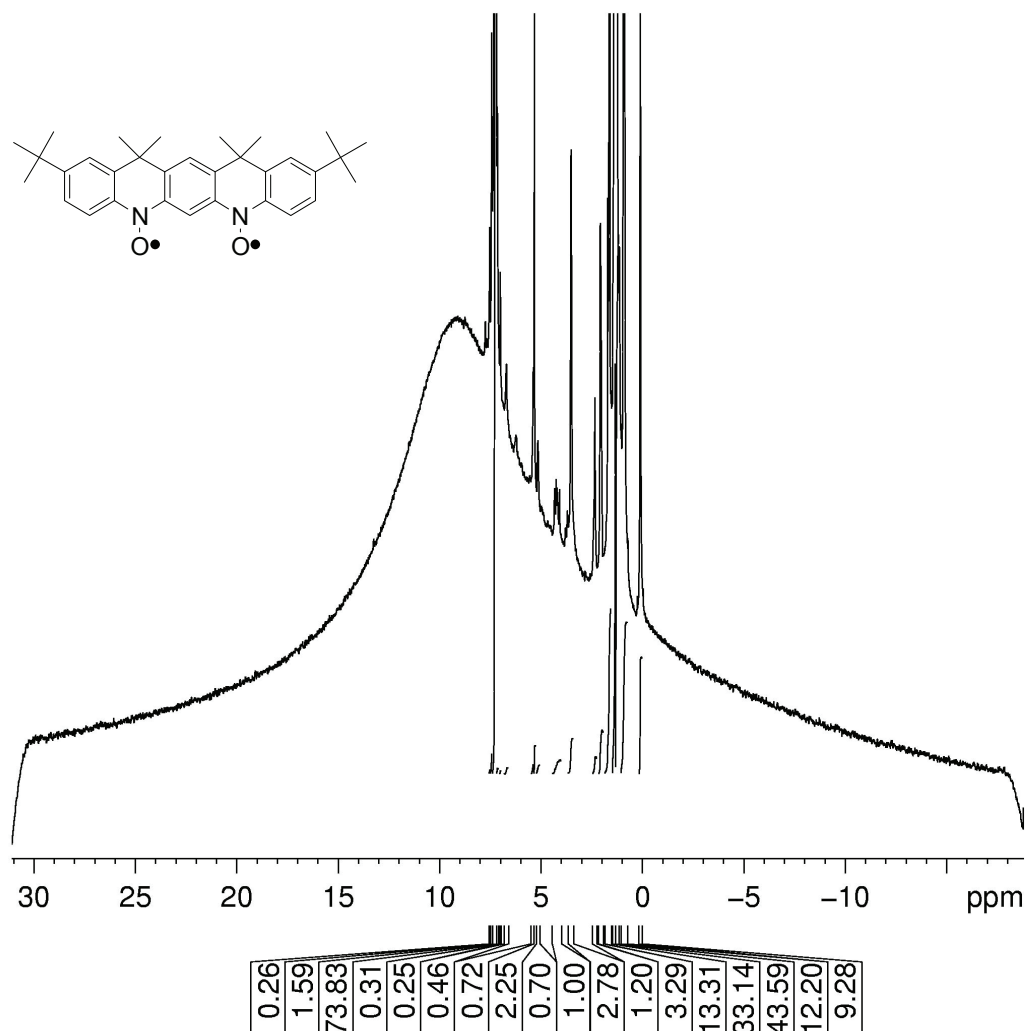

Figure S10b. ^{1}H NMR (400 MHz, CDCl₃) spectrum of nitroxide diradical **2** (KS357-3).

ks-03-057-3 total Integration set = 1000
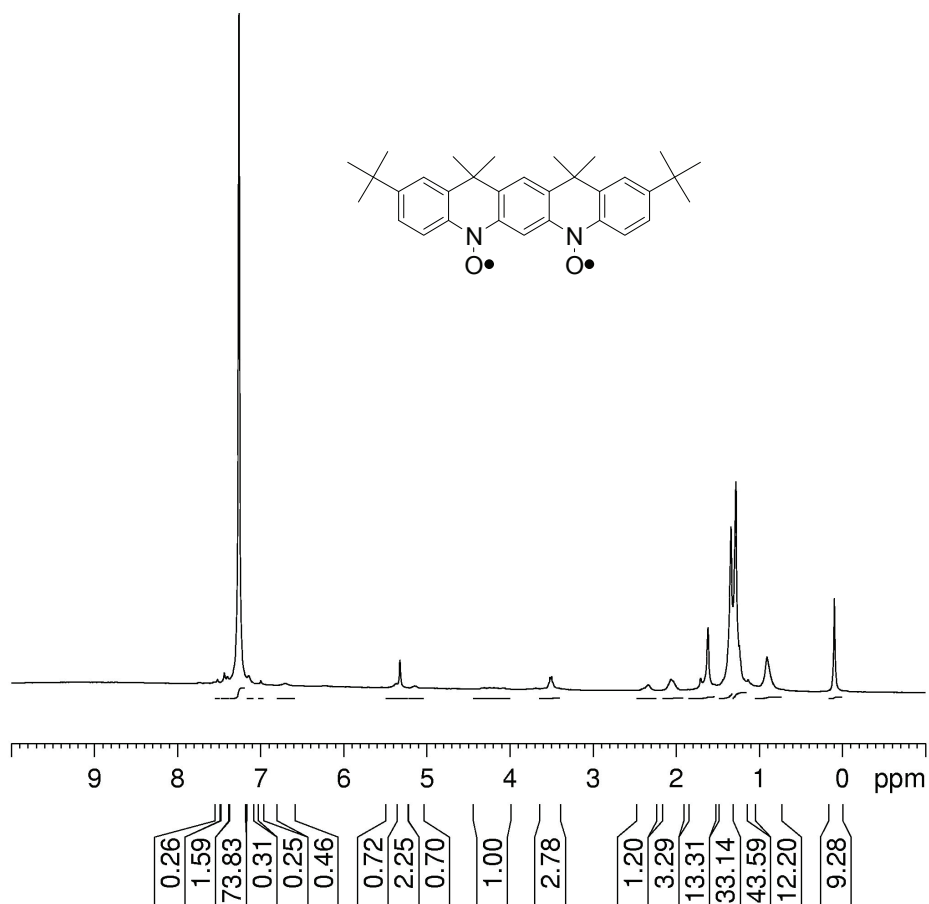
Figure S10c. ^{1}H NMR (400 MHz, CDCl$_3$) spectrum of nitroxide diradical **2** (KS357-3); solvent

and diamagnetic impurities.
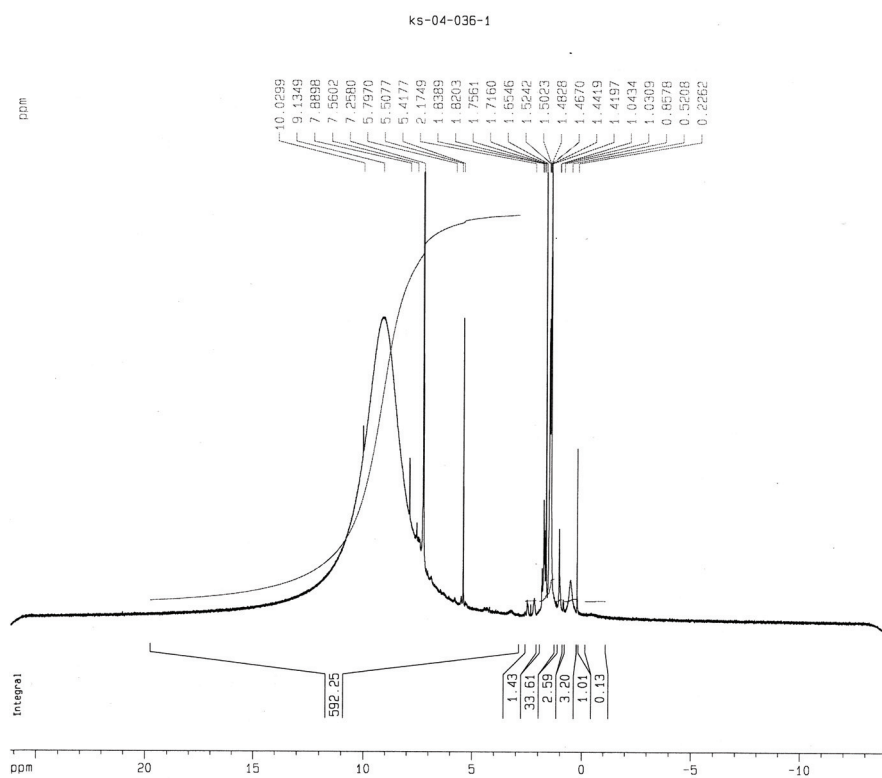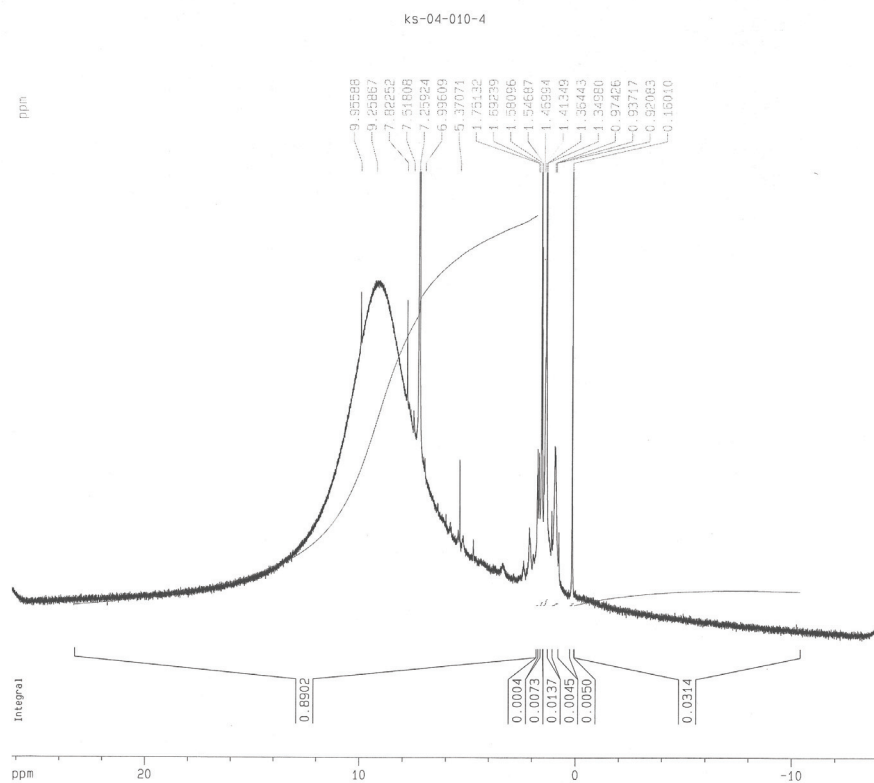
Figure S11. ^{1}H NMR (400 MHz, CDCl$_3$) spectra of representative samples of nitroxide diradical

2 (sample labels: KS410-4 and KS436-1, Table S2).

KS450-1r1 in heptane (Notebook; KS1262, 2.69x10-5M)
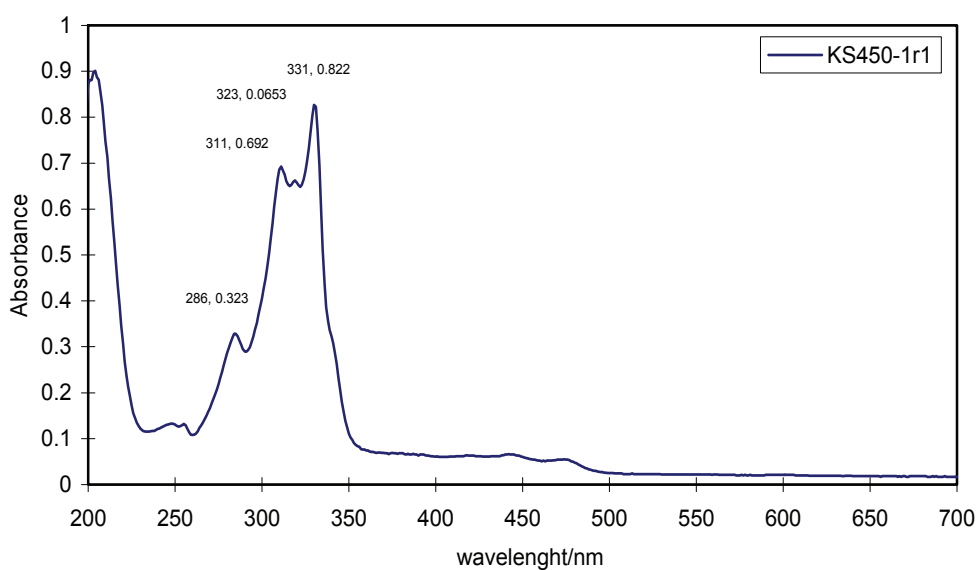
KS450-1r1 in heptane (Notebook; KS1262, 2.69x10-5M)
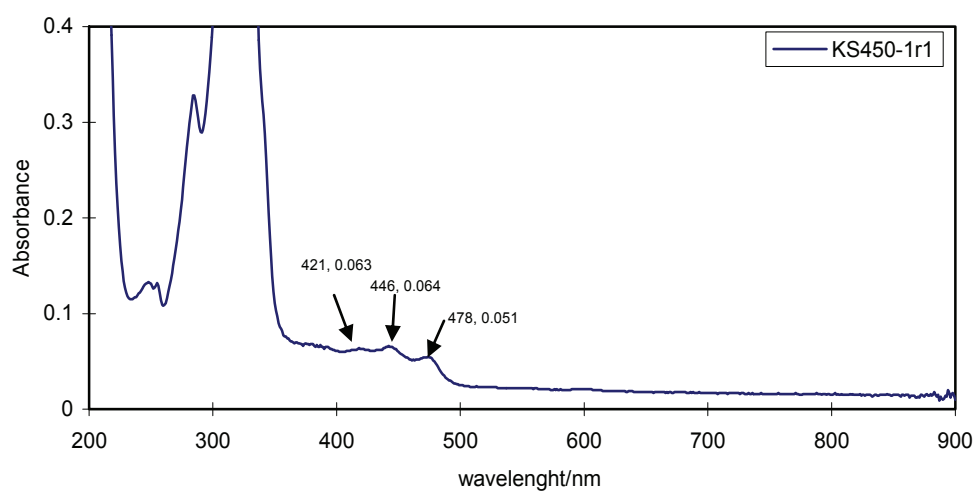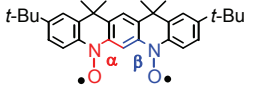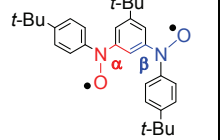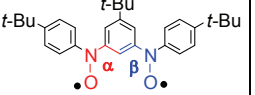
nm	Abs.	ε
286	0.323	5.1E+03
311	0.692	1.1E+04
323	0.653	1.0E+04
331	0.822	1.3E+04
421	0.063	1.0E+03
446	0.064	1.0E+03
323	0.051	0.8E+03

Figure S12. UV-vis electronic absorption spectrum of 2.7×10^{-5} M nitroxide diradical **2** (sample

label: KS450-1) in heptane (KS1262).

9. DFT calculations.

Table S3. Summary of UB3LYP/6-31G(d) calculations for diradical **2**, and for the anti- and endo-conformers of the previously reported diarylnitroxide diradical **1**.[S3]

	2	**1-anti**	**1-endo**
Optimized geometry for triplets			
N…N, O…O distances (Å) for triplets	4.8, 4.7	4.9, 6.2	4.8, 4.9
α, β torsion angles (°) for triplets	0.0, 0.0	25.2, 154.3	26.6, 26.3
Dipole moment[a] for triplets	6.31	2.87	5.51
Total energy for triplets (^{T}E)[b]	−1502.16836909	−1425.92486953	−1425.92309079
Relative energy for triplets[c]	-	0	1.11
Zero-point-energy (ZPE) for triplets[c]	397.39467	388.646	388.589
Lowest vibrational frequencies	13.3, 27.8, 30.1		
Total energy for BS singlets ($^{S}E_{BS}$), triplet geom[b,d,e]	−1502.16676111	−1425.92343452	−1425.92187961
Total energy for BS singlets ($^{S}E_{BS}$), optimized[b,d,e]	−1502.16681855		
ZPE for BS singlets[c]	397.42476		
Lowest vibrational frequencies for BS singlets	13.3, 26.9, 30.2		
$2(^{S}E_{BS} - {}^{T}E)$[c,e], at the triplet geometries	2.02	1.8	1.5
$2(^{S}E_{BS} - {}^{T}E)$[c,e], at the optimized geometries, with no ZPE correction	1.95		
$2(^{S}E_{BS} - {}^{T}E)$[c,e], at the optimized geometries, after ZPE	2.01		

[a] Dipole moment in Debeye. [b] in Hartree/molecule. [c] in kcal mol^{-1}. [d] Broken-symmetry singlet with $S(S + 1) \approx 1.0$ at the geometry optimized for the triplet. [e]The UB3BLYP (broken symmetry with $S(S + 1) \approx 1.0$ singlets and $S(S + 1) \approx 2.0$ triplets) level of theory usually overestimates the singlet-triplet gaps, $2(^{S}E_{BS} - {}^{T}E)$, for the triplet ground state organic diradicals, and underestimates such gaps for the singlet ground state diradicals.[S6-S8]

Nitroxide diradical 2, triplet: geometry optimization and frequency calculation.

Stoichiometry   C32H38N2O2(3)
 Framework group   C1[X(C32H38N2O2)]
 Deg. of freedom   216
 Full point group   C1
 Largest Abelian subgroup   C1   NOp   1
 Largest concise Abelian subgroup C1   NOp   1
                              Standard orientation:

| Center | Atomic | Atomic | Coordinates (Angstroms) | | |
| Number | Number | Type | X | Y | Z |

1	7	0	2.400715	1.864027	0.000000
2	7	0	-2.400715	1.864027	0.000000
3	6	0	6.224738	0.048421	-0.000003
4	6	0	5.053388	-0.723554	-0.000003
5	1	0	5.148647	-1.804895	-0.000003
6	6	0	3.764998	-0.179989	-0.000002
7	6	0	2.539198	-1.100758	-0.000002
8	6	0	1.236222	-0.295983	-0.000001
9	6	0	0.000000	-0.949787	-0.000001
10	1	0	0.000000	-2.034859	-0.000002
11	6	0	-1.236222	-0.295983	0.000000
12	6	0	-2.539198	-1.100758	0.000000
13	6	0	-3.764998	-0.179989	0.000000
14	6	0	-5.053388	-0.723554	0.000000
15	1	0	-5.148647	-1.804895	0.000000
16	6	0	-6.224738	0.048421	0.000002
17	6	0	-6.068141	1.442777	0.000002
18	1	0	-6.933986	2.094701	0.000003
19	6	0	-4.808222	2.025013	0.000002
20	1	0	-4.681240	3.100063	0.000002
21	6	0	-3.661208	1.222000	0.000001
22	6	0	-1.207025	1.113274	0.000000
23	6	0	0.000000	1.812727	0.000000
24	6	0	1.207025	1.113274	0.000000
25	6	0	3.661208	1.222000	-0.000002
26	6	0	4.808222	2.025013	-0.000002
27	6	0	6.068141	1.442777	-0.000002
28	1	0	6.933986	2.094700	-0.000003
29	6	0	7.600026	-0.642790	0.000000
30	6	0	7.734816	-1.527508	-1.262411
31	1	0	6.961540	-2.302031	-1.303128
32	1	0	8.709888	-2.029667	-1.273371
33	1	0	7.652532	-0.925007	-2.174140
34	6	0	8.760832	0.370665	-0.000010
35	1	0	8.742628	1.012822	0.887842
36	1	0	8.742618	1.012815	-0.887867
37	1	0	9.717003	-0.164591	-0.000007
38	6	0	7.734817	-1.527483	1.262430
39	1	0	6.961547	-2.302012	1.303158
40	1	0	7.652524	-0.924967	2.174148
41	1	0	8.709893	-2.029634	1.273405
42	6	0	2.580127	-1.996583	-1.268440
43	1	0	2.551990	-1.385335	-2.176048
44	1	0	1.726682	-2.681962	-1.292469

45	1	0	3.492461	-2.600959	-1.292917
46	6	0	2.580126	-1.996579	1.268440
47	1	0	2.551985	-1.385328	2.176045
48	1	0	3.492460	-2.600953	1.292919
49	1	0	1.726681	-2.681958	1.292468
50	6	0	-2.580127	-1.996580	-1.268440
51	1	0	-2.551988	-1.385331	-2.176047
52	1	0	-3.492462	-2.600954	-1.292918
53	1	0	-1.726683	-2.681960	-1.292469
54	6	0	-2.580126	-1.996581	1.268440
55	1	0	-2.551986	-1.385332	2.176046
56	1	0	-1.726680	-2.681960	1.292468
57	1	0	-3.492459	-2.600957	1.292918
58	6	0	-7.600026	-0.642790	0.000002
59	6	0	-7.734820	-1.527490	-1.262422
60	1	0	-6.961548	-2.302016	-1.303150
61	1	0	-7.652531	-0.924976	-2.174144
62	1	0	-8.709895	-2.029643	-1.273392
63	6	0	-7.734814	-1.527502	1.262418
64	1	0	-7.652525	-0.924997	2.174144
65	1	0	-6.961539	-2.302026	1.303136
66	1	0	-8.709887	-2.029659	1.273384
67	6	0	-8.760832	0.370665	0.000003
68	1	0	-9.717003	-0.164591	0.000003
69	1	0	-8.742624	1.012817	-0.887853
70	1	0	-8.742621	1.012819	0.887856
71	1	0	0.000000	2.892454	0.000000
72	1	0	4.681240	3.100063	-0.000001
73	8	0	2.344869	3.143443	0.000000
74	8	0	-2.344869	3.143443	0.000001

Rotational constants (GHZ):   0.3571653   0.0408679   0.0378921
Standard basis: 6-31G(d) (6D, 7F)

SCF Done: E(UB+HF-LYP) =   -1502.16836909   A.U. after   22 cycles
            Convg   =   0.2662D-08   -V/T =   2.0096
            S**2   =   2.0375
Annihilation of the first spin contaminant:
S**2 before annihilation   2.0375,   after   2.0009

Item	Value	Threshold	Converged?
Maximum Force	0.000001	0.000015	YES
RMS Force	0.000000	0.000010	YES
Maximum Displacement	0.000039	0.000060	YES
RMS Displacement	0.000008	0.000040	YES

Predicted change in Energy = -2.169509D-11
Optimization completed.
    -- Stationary point found.

After frequency calculation:

Item	Value	Threshold	Converged?
Maximum Force	0.000000	0.000015	YES
RMS Force	0.000000	0.000010	YES
Maximum Displacement	0.000029	0.000060	YES
RMS Displacement	0.000006	0.000040	YES

Predicted change in Energy=-5.565784D-12
Optimization completed.
    -- Stationary point found.

Nitroxide diradical 2, BS singlet: geometry optimization and frequency calculation.

Stoichiometry   C32H38N2O2
Framework group   C1[X(C32H38N2O2)]
Deg. of freedom   216
Full point group   C1
Largest Abelian subgroup   C1   NOp   1
Largest concise Abelian subgroup C1   NOp   1

Standard orientation:

Center Number	Atomic Number	Atomic Type	Coordinates (Angstroms)		
			X	Y	Z
1	7	0	-2.404684	1.864709	0.000000
2	7	0	2.404684	1.864709	0.000000
3	6	0	-6.225610	0.046541	0.000000
4	6	0	-5.053211	-0.723862	-0.000001
5	1	0	-5.147164	-1.805361	-0.000001
6	6	0	-3.765626	-0.178632	-0.000001
7	6	0	-2.538492	-1.097310	-0.000001
8	6	0	-1.235586	-0.292254	-0.000001
9	6	0	0.000000	-0.947295	0.000000
10	1	0	0.000000	-2.032238	0.000000
11	6	0	1.235586	-0.292254	0.000000
12	6	0	2.538492	-1.097310	0.000000
13	6	0	3.765626	-0.178632	0.000000
14	6	0	5.053211	-0.723862	0.000001
15	1	0	5.147164	-1.805361	0.000001
16	6	0	6.225610	0.046541	0.000001
17	6	0	6.070485	1.441243	0.000000
18	1	0	6.937204	2.092043	0.000000
19	6	0	4.811622	2.025343	0.000000
20	1	0	4.686497	3.100637	0.000000
21	6	0	3.662921	1.223828	0.000000
22	6	0	1.205297	1.114174	0.000000
23	6	0	0.000000	1.814007	0.000000
24	6	0	-1.205297	1.114174	0.000000
25	6	0	-3.662921	1.223828	0.000000
26	6	0	-4.811622	2.025343	0.000000
27	6	0	-6.070485	1.441243	0.000000
28	1	0	-6.937204	2.092043	0.000000
29	6	0	-7.600057	-0.646314	0.000001
30	6	0	-7.733978	-1.531215	1.262384
31	1	0	-6.959742	-2.304789	1.303128
32	1	0	-8.708430	-2.034605	1.273331
33	1	0	-7.652436	-0.928616	2.174116
34	6	0	-8.762023	0.365818	0.000000
35	1	0	-8.744494	1.008004	-0.887847
36	1	0	-8.744493	1.008006	0.887846
37	1	0	-9.717620	-0.170474	0.000002
38	6	0	-7.733980	-1.531217	-1.262381
39	1	0	-6.959744	-2.304791	-1.303126
40	1	0	-7.652440	-0.928620	-2.174114
41	1	0	-8.708431	-2.034607	-1.273326
42	6	0	-2.577785	-1.993092	1.268622
43	1	0	-2.549496	-1.381710	2.176121
44	1	0	-1.724374	-2.678495	1.292364

45	1	0	-3.490109	-2.597343	1.293390
46	6	0	-2.577784	-1.993091	-1.268625
47	1	0	-2.549495	-1.381708	-2.176123
48	1	0	-3.490109	-2.597342	-1.293393
49	1	0	-1.724373	-2.678494	-1.292367
50	6	0	2.577784	-1.993092	1.268624
51	1	0	2.549495	-1.381709	2.176122
52	1	0	3.490108	-2.597342	1.293392
53	1	0	1.724373	-2.678494	1.292366
54	6	0	2.577785	-1.993092	-1.268623
55	1	0	2.549496	-1.381709	-2.176122
56	1	0	1.724374	-2.678495	-1.292365
57	1	0	3.490109	-2.597343	-1.293391
58	6	0	7.600057	-0.646314	0.000000
59	6	0	7.733979	-1.531217	1.262382
60	1	0	6.959743	-2.304791	1.303127
61	1	0	7.652439	-0.928620	2.174115
62	1	0	8.708431	-2.034607	1.273327
63	6	0	7.733979	-1.531215	-1.262383
64	1	0	7.652437	-0.928616	-2.174115
65	1	0	6.959742	-2.304789	-1.303128
66	1	0	8.708430	-2.034605	-1.273330
67	6	0	8.762023	0.365818	0.000001
68	1	0	9.717620	-0.170474	0.000000
69	1	0	8.744494	1.008004	0.887848
70	1	0	8.744493	1.008006	-0.887845
71	1	0	0.000000	2.893618	0.000000
72	1	0	-4.686497	3.100637	0.000001
73	8	0	-2.344126	3.144340	0.000000
74	8	0	2.344126	3.144340	0.000000

Rotational constants (GHZ):   0.3571836   0.0408627   0.0378880
Standard basis: 6-31G(d) (6D, 7F)
SCF Done: E(UB+HF-LYP) =   -1502.16681863   a.u. after   2 cycles
             Convg   =   0.1986D-05   18 Fock formations.
               S**2 =   1.0127   -V/T =   2.0096
Annihilation of the first spin contaminant:
S**2 before annihilation   1.0127,   after   0.1575

Item	Value	Threshold	Converged?
Maximum Force	0.000000	0.000015	YES
RMS Force	0.000000	0.000010	YES
Maximum Displacement	0.000005	0.000060	YES
RMS Displacement	0.000001	0.000040	YES

Predicted change in Energy=-3.141572D-13
Optimization completed.
    -- Stationary point found.

After frequency calculation:

Item	Value	Threshold	Converged?
Maximum Force	0.000000	0.000015	YES
RMS Force	0.000000	0.000010	YES
Maximum Displacement	0.000005	0.000060	YES
RMS Displacement	0.000001	0.000040	YES

Predicted change in Energy=-3.289080D-13
Optimization completed.
    -- Stationary point found.

10. Supporting references.

S1. W. Adam, J. Bialas and L. Hadjiarapoglou, *Chem. Ber.*, 1991, **124**, 2377.

S2. M. Gilbert, M. Ferrer, F. Sanchez-Baeza and A. Messeguer, *Tetrahedron*, 1997, **53**, 8643–8650.

S3. A. Rajca, M. Vale and S. Rajca, *J. Am. Chem. Soc.*, 2008, **130**, 9099–9105.

S4. A. Rajca, M. Takahashi, M. Pink, G. Spagnol and S. Rajca, *J. Am. Chem. Soc.*, 2007, **129**, 10159–10170.

S5. A. Rajca, S. Mukherjee, M. Pink and S. Rajca, *J. Am. Chem. Soc.*, 2006, **128**, 13497–13507.

S6. D. Y. Zhang, D. A. Hrovat, M. Abe and W. T. Borden, *J. Am. Chem. Soc.*, 2003, **125**, 12823–12828.

S7. C. J. Cramer and B. A. Smith, *J. Phys. Chem.*, 1996, **100**, 9664–9670.

S8. A. H. Winter, D. E. Falvey, C. J. Cramer and B. F. Gherman, *J. Am. Chem. Soc.*, 2007, **129**, 10113–10119